PERGAMON

International Journal of Heat and Mass Transfer 44 (2001) 2511–2521

International Journal of HEAT and MASS TRANSFER

www.elsevier.com/locate/ijhmt

Experimental investigation of natural convective heat transfer from a round plate of complex configuration

V.V. Vlassov [a,*], G.A. Dreitser [b]

[a] Division of Space Mechanics and Control, National Institute for Space Researches (INPE), 12227-010 S.J. Campos, SP, Brazil
[b] Department of Aviation-Space Thermal Techniques, Moscow State Aviation Institute (MAI), 125871 Moscow, Russian Federation

Received 26 July 2000

Abstract

Experimental results of free convective heat transfer on a round plate with additional elements on the surface at ambient air temperatures are presented. The tests were performed at horizontal and vertical positions of the plate. The influence of an annular non-heated barrier and partial upper insulation was studied. Experimental data were obtained at steady-state and transient modes over the Rayleigh number range from 1×10^7 to 2×10^8. Validity of the quasi-steady-state postulation for transient heat transfer was evaluated. Results were reduced to power-type relations $Nu = f(Ra)$ and compared with the known steady-state data for free convection over smooth surfaces.

1. Introduction

Problems of heat transfer under free convection are being permanently studied widely over the world due to their application importance in the area of cooling of electronics. Most of these investigations were performed for flat surfaces completely involved in the heat transfer [1,2]. Some particular cases of practical interest of heat transfer by free convection at surfaces of complex configuration (i.e. presence of convexities or cavities, non-heated sections and lateral barriers) were studied experimentally and numerically. Because of a large variety of cases the generalization of data is complicated by virtue of insufficient investigations, despite great practical interest. Each case should be studied separately to be compared with respect to applicability of relations obtained for classic flat surfaces.

Many studies have been devoted to discover the natural convection phenomena of surface partial heating. Investigations of a vertical surface with a partially heated bottom section [3–6] show that the flow patterns as well as heat transfer coefficients were practically the same as for the case of flat plates for entire heating. The same was seen for the condition of partial heating top section. On the other hand, experimental study of natural convection from a heat module, mounted on a horizontal surface, indicates very different temperature distributions [7]. If a heated surface looks upward, partial heating facilitates the process of stabilizing of convective cells. Therefore, as demonstrated in [8,9], heat transfer to the whole area of a plate was higher than for homogeneous heating under the same value of total heat flux. In [8] it was obtained that under laminar convection with the heated-to-cold strip width reduction the heat transfer increases. Localization of a heater into the central region of a plate also caused heat transfer to increase. No investigations were carried out for ring-type unheated zones on a circular plate.

In [10–13] natural convection heat transfer over a horizontal plate bounded by vertical walls was considered. In [10], it was shown that under laminar flow at $Ra = 10^5$ to 10^7 the vertical barriers increased heat transfer from 50% to 7%, respectively. In [11–13], it was shown that in the region of progressed turbulent flow the altering of the lateral barrier height had weak influence on intensity of heat transfer on a horizontal surface. At the same time the comparison of the data obtained in [11] with those for a plate without barriers showed that these barriers cannot only increase but also decrease heat transfer under $Gr_L = 10^4 \div 10^7$ at different boundary conditions ($q_w = \text{const}$ or $T_w = \text{const}$).

* Corresponding author.

0017-9310/01/$ - see front matter
PII: S0017-9310(00)00275-1

Nomenclature

A	area
a	thermal diffusivity
b	coefficient of approximation
Bi	Biot number, $\alpha L/\lambda_w$
C	specific heat
D	diameter
G	Gebhart factor
Gr	Grashof number, $(g\beta_m(T_w - T_\infty)D^3)/v_m^2$
g	gravity acceleration
L	length
Nu	Nusselt number, $\alpha D/\lambda_m$
Pr	Prandtl number, v_m/a_m
Q	heat flux
q	heat flux density
r	contact thermal resistance
Ra	Rayleigh number $(g\beta_m(T_w - T_\infty)D^3)/(v_m a_m)$
T	temperature
t	time
Zh	Zhukovsky number, tv/L^2

Greek symbols

α	heat transfer coefficient
β	eigenvalue
δ	thickness or variation
ε	emissivity
η	correction factor
φ	coefficient
λ	thermal conductivity
v	kinematic viscosity
ρ	density
σ	Stefan–Boltzmann constant

Subscripts

cr	critical
D	diameter
IR	infrared
L	length
m	average or numeric index
s	bottom insulation
ss	steady state
u	upper insulation
w	wall of the base plate
∞	ambient

Horizontal ribs of poor conduction can even be used for suppressing free convection from a flat vertical plate [14]. The ratio is higher for top barriers than for bottom ones [15,16]. At the top region of the plate in the vicinity of the barrier in the conditions of laminar flow convective heat transfer reduces considerably by 40–80% [15]. If the flow is turbulent, then the reduction is not more than 13%.

Local heat transfer coefficients were measured on six circular thin polished brass sheets of the diameter within 100 to 500 mm [17]. Edge effects were investigated. The interaction of free convection and radiation was studied for a single fin [18] and in a partitioned enclosure [19].

The present work is devoted to the experimental investigation of convective heat transfer under free convection in air on a heated high-conductivity thick round plate with two round openings. The surface is treated as black therefore the radiative heat transfer is also taken into account. This investigation has been extracted from a practical problem on defining thermal requirements for ground electrical tests and verifications of a Brazilian Space experiment named CIMEX to be flown as a payload of the Gas Away Special Program onboard Space Shuttle. The plate simulates a radiator plate of the optical block detector assembling used for heat removal from an internal mechanical cryocooler and a box of electronics. The experiment operates in periodic mode (switch-on–switch-off), therefore the investigations of steady-state and unsteady variations of heat transfer coefficient is very important for determining the thermal limits of ground test operation and standby periods.

2. Test setup

A radiator simulator is a round plate made of an aluminum alloy ($C_w\rho_w = 2.33 \times 10^6$ J/°C/m^3) of 9.0 ± 0.05 mm thickness and 384 ± 0.3 mm dia. Two round openings 103.8 mm in dia. are placed, as shown in Fig. 1. Cylindrical pieces of insulation of 36 mm height are inserted in these openings for physical simulation of the baffles of the optical detectors. The radiator surface has been treated by deep black anodizing with emissivity of $\varepsilon_w = 0.915 \pm 0.0022$ measured by the reflectivity method in the infrared band. The radiator surface is partly covered by an upper foam plastic insulated ring to simulate a vacuum multi-layer insulation. The radiator surface opening that is not covered by an upper insulation is 293 ± 0.5 mm in dia. The thickness of the upper insulation is 9.5 ± 0.3 mm, measured emissivity -0.685 ± 0.009 and density -12.0 ± 0.1 kg/m^3. Diameter of the experimental package assembling is 504 ± 1 mm.

Six skin electrical heaters are glued on the inner surface of the plate. The maximum total heating power is limited to 24 W and distributed in such a way to provide uniform heat flux density to each heater. The generated heat is rejected from the upper surface of the plate by natural convection and radiation.

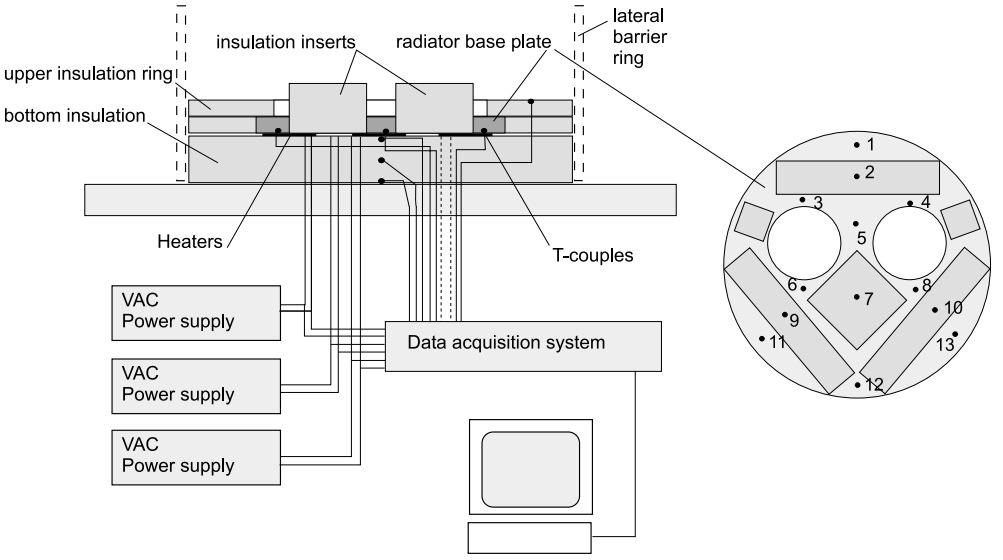

Fig. 1. Experimental set-up and lay-out of heaters and thermocouples.

The thermocouples of T-type (Cu–constantan) are distributed over the inner surface of the base plate. Four of them are located between the base plate and heaters, whereas the other nine are placed in the vicinity of the heaters. Thermocouple junctions 1.0 mm in dia. are put into small cavities to reach good thermal contact. Thermocouple wires are in thermal contact with the plate through electrical insulation.

Rear surface of the plate is covered with a foam plastic of the same type and of 39 ± 0.4 mm thickness. The thermocouples were also installed over the outer surfaces of insulation to estimate heat losses.

The following values were being scanned at 30 s intervals: voltage on heaters, temperatures at 13 points of the inner base-plate surface, temperatures at the outer insulation surfaces, ambient air temperature.

3. Experimental data reduction for a steady state

Heat flux removal from the outer surface of the plate by natural convection is determined from the energy balance. Radiation heat transfer and heat losses to insulation are considered. Lateral heat losses are assumed as being insignificant. The heat transfer coefficient at steady state can be expressed through the following equation:

$$\alpha_{ss} = \frac{q_w - \varphi q_{IR} - q_s - (1-\varphi)q_u}{(T_w - T_\infty)\varphi}, \tag{1}$$

where q_w is the heating power density and $\phi = 1 - A_u/A_w$.

The parameter φ was introduced to distinguish two experimental configurations: case A – presence of the upper insulation ring and case B – absence of it ($\varphi = 1$).

Heat losses through the bottom insulation q_s and upper insulation ring q_u are defined as

$$q_s = \frac{\lambda_s}{\delta_s}(T_w - T_{s^*}), \qquad q_u = \frac{\lambda_s}{\delta_u}(T_w - T_{u^*}), \tag{2}$$

where T_{s^*} and T_{u^*} are the measured temperatures on the outer insulation surfaces.

Heat flux by radiation

$$q_{IR} = \varepsilon_w \sigma \eta \left(T_w^4 - T_\infty^4\right). \tag{3}$$

Coefficient η is a correction factor for effective area of heat transfer due to radiative interaction with conjugated parts of insulation and surrounding walls of the hall of experimental site. Its value has been obtained from the solution of an appropriate sub-problem of net radiative heat transfer in a closed enclosure composed of the three generalized surfaces – the radiator plate itself, the insulation inserts with upper ring, and the hall walls. Angle factors have been calculated by the Monte-Carlo methods with a precision of 0.002% whereas the η coefficient expressed via Gebhart factor as $\eta = 1 - G_{ww}$ was found using the Gebhart technique [20]. With the emissivities $\varepsilon_s = 0.685 \pm 0.009$, $\varepsilon_w = 0.910 \pm 0.09$ and taking into account uncertainties in the calculation of angle factors and areas of surrounded walls, the obtained values are the following: $\eta = 0.9872 \pm 0.00065$ (case A) and $\eta = 0.9914 \pm 0.00065$ (case B).

The average temperature of the plate inner surface is defined as a simple mean of measured values at 13 points. The average temperature of the outer surface of the base plate T_w is very close to the inner one and the maximal difference is not higher than 0.002°C. The

Nusselt, Grashof, Rayleigh, and Prandtl numbers are determined at average temperatures $T_m = 0.5(T_w + T_\infty)$ and taking the diameter of open surface of the base plate, that differs for the cases A and B, as a reference.

4. Data reduction technique for transient tests

Due to poor heat transfer and high thermal inertia of the plate, heat loss to the insulation has to be treated carefully. Due to the high conductivity of the plate, the thermal gradient in it can be neglected. Fig. 2 shows a 1D assumption of the experiment conditions. A composite model consists of a lumped model of the base plate and one-dimensional distributed models for each insulation plate. The set of the energy equations can be written for three media – the plate itself (subscript w) and two insulating plates, bottom (s) and upper (u) ones:

$$\begin{aligned} C_w\delta_w\rho_w\frac{dT_w}{dt} &= q_0(t) - \alpha\varphi(T_w - T_\infty) - \varepsilon\eta\sigma\varphi\left(T_w^4 - T_\infty^4\right) \\ &\quad - \lambda_s\frac{\partial T_s}{\partial x}\bigg|_{x=x_1} + (1-\varphi)\lambda_u\frac{\partial T_u}{\partial x}\bigg|_{x=x_2}, \\ C_s\rho_s\frac{\partial T_s}{\partial t} &= \frac{\partial}{\partial x}\left[\lambda_s\frac{\partial T_s}{\partial x}\right], \\ C_u\rho_u\frac{\partial T_u}{\partial t} &= \frac{\partial}{\partial x}\left[\lambda_u\frac{\partial T_u}{\partial x}\right]. \end{aligned} \tag{4}$$

Conjugate and boundary conditions:

$$\begin{aligned} &x = 0 : \lambda_s\frac{\partial T_s}{\partial x} = r^{-1}(T_s - T_\infty), \\ &x = x_1 : T_s = T_w, \\ &x = x_2 : T_u = T_w, \\ &x = x_3 : -\lambda_u\frac{\partial T_u}{\partial x} = \alpha(T_u - T_\infty) + \varepsilon_u\sigma\left(T_u^4 - T_\infty^4\right). \end{aligned} \tag{5}$$

It is accepted that all transient tests consist of two phases, first – heating at constant heat dissipation and second - cooling by natural convection with heaters switched off at time t_1. Under such conditions, the heat flux can be defined through a step-function, $q_w(t) = [1 - U(t - t_1)]Q/A_w$.

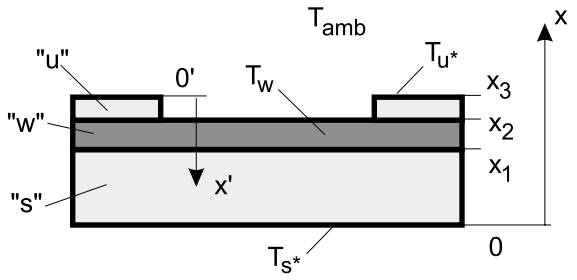

Fig. 2. Idealization of the experiment conditions.

The first equation of set (4) could be solved separately if spatial derivatives are known. These derivatives can be extracted from the transient temperature profiles over the insulation plates. To achieve the decomposition of the equation set (4), the measured temperatures on the outer surfaces of the each insulation are utilized. Polynomial approximation of $n = 3$th up to 7th power is used to smooth experimental data contained from 400 to 700 records: $\tilde{T}_i(t) = \mathrm{pol}_n[\hat{T}_i(t)]$.

A modification of boundary conditions can be accomplished under the assumption that the ambient temperature is constant throughout two phases of each test that is very close to reality. Thus, under this assumption, the boundary and conjugate conditions become the following:

$$\begin{aligned} &x = 0 : \Delta\tilde{T}_s = \tilde{T}_{s^*}(t) - T_\infty(0), \\ &x = x_1 : \Delta\tilde{T}_s = \tilde{T}_w(t) - T_\infty(0), \\ &x = x_2 : \Delta\tilde{T}_u = \tilde{T}_w(t) - T_\infty(0), \\ &x = x_3 : \Delta\tilde{T}_u = \tilde{T}_{u^*}(t) - T_\infty(0). \end{aligned} \tag{6}$$

The last two equations of set (4) should be rewritten in new variables ΔT_i instead of T_i.

Thus, initial conditions under such modifications are homogeneous, if each test begins with all the temperatures equal to ambient. The exact analytical solution for this kind of problem under conditions (6) is available in literature [25,26]. The solution is obtained by using Green's functions and afterwards modified by integration two times by parts to avoid divergence on boundaries.

A closed-form relation for the bottom insulation transient profiles is expressed in terms of primal variables

$$\begin{aligned} T_s(x,t) = &\left(1 - \frac{x}{\delta_s}\right)\tilde{T}_{s^*}(t) + \frac{x}{\delta_s}\tilde{T}_w(t) - \frac{2}{\delta_s}\sum_{m=1}^{\infty}\frac{\sin\beta_m x}{\beta_m} \\ &\times\left\{\left[\left(\tilde{T}_{s^*}(t) - T_\infty(0)\right) - a_s\beta_m^2 I_m(\tilde{T}_{s^*})\right]\right. \\ &\left. - (-1)^m\left[\left(\tilde{T}_w(t) - T_\infty(0)\right) - a_s\beta_m^2 I_m(\tilde{T}_w)\right]\right\}, \end{aligned} \tag{7}$$

where eigenvalues $\beta_m = m\pi/\delta_s$.

As assumed the tests will consist of two phases initiating from uniform ambient temperatures. The first phase is heating with power switched on and second one is cooling at power switched off. The integral function is defined as follows:

$$\begin{aligned} I_m(\tilde{T}) &= \int_0^t\left[\tilde{T}(\tau - t_1 U(\tau - t_1)) - T_\infty(0)\right]e^{-a_s\beta_m^2(t-\tau)}\,d\tau \\ &= \int_0^{t_1}\left[\tilde{T}(\tau) - T_\infty(0)\right]e^{-a_s\beta_m^2(t-\tau)}\,d\tau \\ &\quad + \int_{t_1}^t\left[\tilde{T}(\tau - t_1) - T_\infty(0)\right]e^{-a_s\beta_m^2(t-\tau)}\,d\tau. \end{aligned} \tag{8}$$

Here the unit step function $U(\cdot)$ reflects the fact that the polynomial smoothing is executed separately for each phase of test, initiating from 0-local time at the phase of cooling, as at heating.

The definite integral of the product of exponent and polynomial for any time interval from t_A to t_B can be obtained in closed analytical form

$$\int_{t_A}^{t_B} \Delta\tilde{T}(\tau)\, \mathrm{e}^{-a_s\beta_m^2(t-\tau)}\, \mathrm{d}\tau = \int_{t_A}^{t_B} \sum_{k=0}^{n} b_k \tau^k\, \mathrm{e}^{-a_s\beta_m^2(t-\tau)}\, \mathrm{d}\tau = \sum_{k=0}^{n-1} b'_k t_B^k + \sum_{k=0}^{n} b''_k t_A^k\, \mathrm{e}^{-a_s\beta_m^2(t_B-t_A)}, \tag{9}$$

where b'_i and b''_i are recursive coefficients, expressed in a reverse order through the primal approximation coefficients b_i:

$$b'_{n-1} = \frac{nb_n}{a_s\beta_m^2}; \quad b'_{k-1} = \frac{k}{a_s\beta_m^2}(b_k - b'_k); \quad k = n-1, \ldots, 1$$
$$b''_n = b_n; \quad b''_{k-1} = b_{k-1} - \frac{k}{a_s\beta_m^2} b''_k; \quad k = n, \ldots, 1. \tag{10}$$

Unknown derivatives in set (4) are obtained directly by differentiation of (7). A final expression for heat flux from the base plate to bottom insulation is compact

$$q_s(t) = \lambda_s \frac{\partial T_s(x,t)}{\partial x}\bigg|_{x=x_1} = \lambda_s \frac{\tilde{T}_w(t) - \tilde{T}_{s^*}(t)}{\delta_s} - \frac{2\lambda_s}{\delta_s} \times \sum_{m=1}^{\infty} \left\{ (-1)^m \left[\left(\tilde{T}_{s^*}(t) - T_\infty(0) \right) - a_s\beta_m^2 I(\tilde{T}_{s^*}) \right] - \left[\left(\tilde{T}_w(t) - T_\infty(0) \right) - a_s\beta_m^2 I(\tilde{T}_w) \right] \right\}. \tag{11}$$

A similar procedure for the top insulation can be performed to define heat flux $q_u(\tau)$ into the top insulation ring using local coordinates (x'), as shown in Fig. 2. The resulting equation is similar to (11) with the differences: $T_{s^*} \to T_{u^*}, \delta_s \to \delta_u$ and $\beta_m \to \beta'_m = m\pi/\delta_u$. The transient value of $\alpha(t)$ is obtained from the first equation of set (4) and finally is expressed analytically as

$$\alpha(t) = \left\{ q_w(t) - C_w\delta_w\rho_w(\mathrm{d}\tilde{T}_w/\mathrm{d}\tau) - \varphi\varepsilon\eta\sigma\left(\tilde{T}_w^4 - \tilde{T}_\infty^4\right) - q_s(t) - (1-\varphi)q_u(t) \right\} \Big/ \left\{ \varphi(\tilde{T}_w - \tilde{T}_\infty) \right\}. \tag{12}$$

The transient Nusselt number is calculated using this value of heat transfer coefficient and diameter of open area of the base plate.

5. Estimation of an experimental uncertainty

The temperature fields through the thickness as well as along the surface of the plate are assumed to be homogeneous due to high conductivity and relatively low thickness of the plate, and also because of low intensity of heat flux. The maximal value of the Biot number is estimated as $Bi = \alpha_\Sigma\delta_w/\lambda_w = 0.0093$ that is less than 0.1, therefore the condition criterion of constant temperature $T_w \cong \text{const}$ through the surface is achieved. It allows to determine merely the average value of the heat transfer coefficient by measurement.

At vertical positioning of the plate the heat transfer coefficient is not homogeneous, but this inhomogeneity will not change the condition of constant temperature; this was confirmed by appropriate evaluations [1,29]. By these data the conjugate parameters are defined as $P_1 = \lambda_w/\lambda_\infty = 4400$ and $P_2 = \lambda_w\delta_w/\lambda_\infty D_w = 114$. For these values, the wall–air heat interaction is very similar to that for a surface with the condition of $T_w = \text{const}$.

The estimation of the experimental uncertainty is related to the level of confidence of 0.97. The error of determination of the heat transfer coefficient under steady-state conditions is defined as the sum of small variations of each parameter, obtained from Eq. (1)

$$\delta\alpha_{ss} = \left| \frac{-Q_w\delta_s\delta_u - A_w\lambda_s(1-\varphi)\Delta T_u\delta_s - \Delta T_s\delta_u}{A_w\Delta T^2\varphi\delta_s\delta_u} \right| \delta\Delta T + \frac{\lambda_s\delta\Delta T_s}{\Delta T\varphi\delta_s} + \frac{\lambda_s(1-\varphi)\delta\Delta T_u}{\Delta T\varphi\delta_u} + \frac{\delta Q_w}{A_w\Delta T\varphi} + \sigma\left(T_\infty^2 + T_w^2\right)(T_\infty + T_w) \cdot | - \eta\delta\varepsilon_w - \varepsilon_w\delta\eta|, \tag{13}$$

where $\Delta T = T_w - T_\infty$.

The error of measurement of temperatures $\delta\Delta T_i$ is defined by the error of thermocouple itself, error of calibration, error of data acquisition and possible deviations related to the thermocouples installation, differences of individual characteristics, etc. These values have probabilistic nature and they are estimated by standard deviations obtained from measured data.

The uncertainty is strongly dependent on the temperature difference ΔT. In accordance with Eq. (13) the reliable data within $\pm 15\%$ can be obtained for steady-state experiments with a temperature difference ΔT exceeding 3.9°C for the case A and 2.0°C for the case B.

In transient tests, the term of enthalpy variation by time in the first equation of set (4) yields a significant contribution to experimental uncertainty. Measured temperatures are smoothed by polynomial approximation, therefore the derivatives are available. The parametric plots of these derivatives versus ΔT under elimination of time are shown in Fig. 3. These data have been extracted from an experiment in horizontal position.

A linear function can approximate the curves in Fig. 3 at maximum average square residual of 1.16×10^{-8}°C^2/s^2, thus in general case

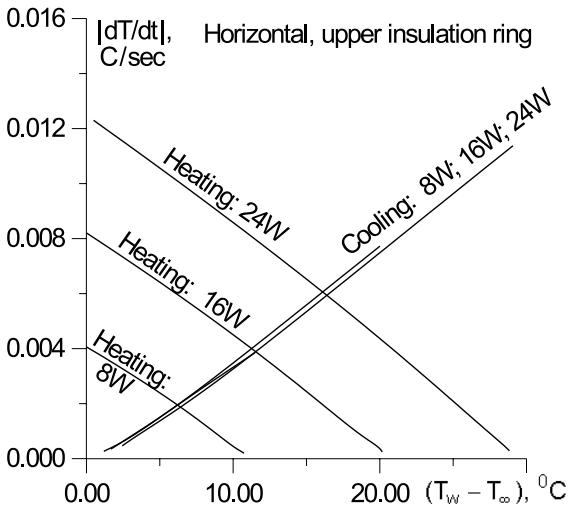

Fig. 3. Velocity of heating/cooling versus temperature difference.

$$\frac{\partial T}{\partial t} \cong b_0 + b_1 \Delta T. \tag{14}$$

Finally transient uncertainty can be estimated after substitution of the Eq. (14) in (12) and subsequent differentiation to obtain an expression in small variations

$$\delta\alpha = \delta\alpha_{ss} + \frac{C_w \rho_w \delta_w b_0}{\Delta T^2 \varphi}\delta\Delta T + \frac{2\lambda_s}{\delta_s \Delta T \varphi}\mathrm{ert}_1(m_1)\delta\Delta T_s + \frac{2\lambda_s(1-\varphi)}{\delta_s \Delta T \varphi}\mathrm{ert}_2(m_1)\delta\Delta T_u. \tag{15}$$

Here ert( ) is an error function of series truncation, expressed as

$$\mathrm{ert}_1(m_1) = \sum_{m=m_1}^{\infty} \chi(m)\, \mathrm{e}^{-a_s \beta_m^2 t}; \qquad \mathrm{ert}_2(m_1) = \sum_{m=m_1}^{\infty} \chi(m)\, \mathrm{e}^{-a_u \beta_m'^2 t}, \tag{16}$$

where $\chi(m) = 1 + (-1)^m$.

The infinite sum in the error functions $\mathrm{ert}_i(\,)$ can be evaluated by the following conservative substitution with respect to the eigenvalues non-linearity:

$$\beta_m \leqslant \frac{\delta_s}{\pi}\beta_m^2 \quad \text{and} \quad \beta'_m \leqslant \frac{\delta_u}{\pi}\beta_m'^2. \tag{17}$$

This substitution allows to obtain closed analytical expressions for an upper limit of truncation errors

$$\mathrm{ert}_1(m_1) \leqslant \left(\mathrm{e}^{-(a_s t\pi^2(m_1-1))/\delta_s^2}\right)\left(\mathrm{e}^{(a_s t\pi^2)/\delta_s^2}\chi(m_1) + \bar{\chi}(m_1)\right)\left(\mathrm{e}^{(2a_s t\pi^2)/\delta_s^2} - 1\right)^{-1}, \tag{18}$$

where $\bar{\chi}(m)$ is a conjugate function with respect to $\chi(m)$, defined as $\bar{\chi}(m) = 1 - (-1)^m$.

For $\mathrm{ert}_2(m_1)$ the relation is similar to (18) with the only difference: δ_u instead of δ_s. For the experimental condition presented the inequality $\mathrm{ert}_2(m_1) < \mathrm{ert}_1(m_1)$ holds elsewhere.

Evaluation at $m_1 = 8$ shows that the defined error-function $\mathrm{ert}_1(m_1)$ has significant value for small times, for example, for $t = 10$ s $\mathrm{ert}_1(8) = 4.43$. But with the time the value decreases drastically. For $t = 1$ min $\mathrm{ert}_1(8) = 0.0166$ whereas for $t = 2$ min $\mathrm{ert}_1(8) = 7.75 \times 10^{-5}$. From experimental data, the maximal developed temperature difference at $t = 2$ min is $\Delta T = 1.9$°C, that is inside the range even of steady-state uncertainty. Therefore, the truncation errors for $m \geqslant 8$ can be neglected.

Uncertainties in the exact definition of the value $(C_w \rho_w \delta_w)$ can be eliminated by introducing a correction factor C_f extracted from the following conjugate conditions: at the instant of switch-off the value of heat transfer coefficient cannot suffer any jump

$$Q(t)/A_w - C_f(C_w\delta_w\rho_w)\left.\frac{\mathrm{d}\tilde{T}_w}{\mathrm{d}\tau}\right|_{t_1-0} = 0 - C_f(C_w\delta_w\rho_w)\left.\frac{\mathrm{d}\tilde{T}_w}{\mathrm{d}\tau}\right|_{t_1+\Delta t}, \tag{19}$$

where Δt is time correction to count a fast time processes across the plate, $\Delta t \approx 0.4$ s [26].

The total uncertainty is strongly dependent on the phase of transient process, i.e. heating or cooling. When heating, the derivative of enthalpy term is high, whereas the temperature difference is still small, thus the accumulation of errors occurs. When cooling, high derivative value is compensated by large values of ΔT, thus no uncertainty increase occurs. As seen from Fig. 3, the parameter of approximation in Eq. (14) at heating phase is $b_0 > 0$ and on cooling $b_0 \approx 0$.

Fig. 4 shows total uncertainties for transient experiments for a heat load of 16 W for both cases of upper insulation, based on test data. For cooling phase, the values are practically equal to incertainties of steady state. For heating phase, they depend on power dissipated. In accordance with (15), experimental data can be accepted as reliable within ±15% when the developed temperature difference ΔT will be higher than the following limit values: Case A – 6.8°C, 8.6°C and 9.6°C; Case B – 4.6°C, 6.2°C and 6.9°C for the power of 8, 16 and 24 W, respectively.

6. Experimental results of steady-state tests

Experiments were carried out over the heating power range from 8 to 24 W; the base-plate temperature was varied from ambient (20–23°C) to 56°C. This supports the Rayleigh number from 1×10^7 up to 2×10^8. Tests

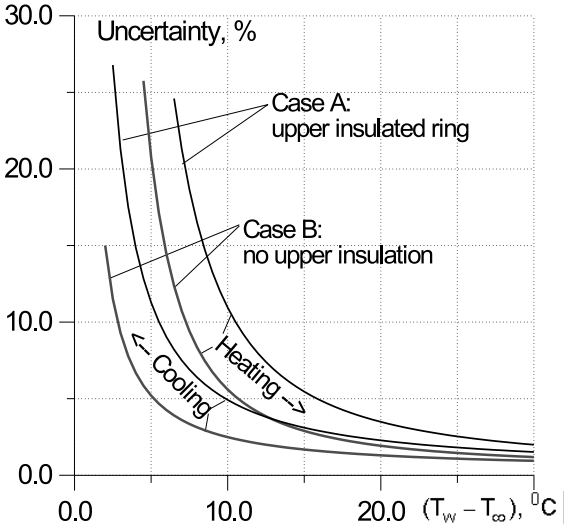

Fig. 4. Estimated uncertainties for a transient experiment at 16 W.

were performed for horizontal and vertical positions of the base plate. For each position, the following configurations were investigated: with and without an upper insulation ring (i.e. the mentioned cases A and B) as well as with and without an annular barrier.

Fig. 5 shows the generalization of the steady-state results obtained for the horizontal position of the plate, for the cases A and B. Experimental points of case A lie very close to the well-known law $0.14Ra^{(1/3)}$ presented by Fishenden [21] for natural turbulent convection at horizontal smooth surfaces, as well as the law $0.15Ra^{(1/3)}$, confirmed in [17] for the thin (0.8 mm) circular brass sheets in the Ra range from 8×10^6 to 3×10^{10}.

The results detect a difference of 22% in the value of heat transfer coefficient between cases A and B. It can be interpreted that the upper insulation ring eliminates some adverse edge effects and simultaneously acts as a turbulizer intensifying convective heat transfer at the perimeter region. On the other hand, the insulation inserts in the central region of the plate interfere development of convective cells, therefore the heat transfer coefficient for the case B is lower than that for smooth horizontal surfaces.

A regression analysis shows that power law for the complex surfaces of presented configuration for turbulent flow is (2/5) rather than (1/3). It can be due to the influence of the insulation inserts at the central region of the base plate.

The best relations obtained for horizontal steady-state experiments are

$$\begin{aligned} Nu_D &= 0.0484\,Ra_D^{(2/5)} \quad \text{(case A)},\\ Nu_D &= 0.0376\,Ra_D^{(2/5)} \quad \text{(case B)}. \end{aligned} \tag{20}$$

Fig. 6 shows the generalization of steady-state results obtained for vertical position of the base plate for all cases of configurations. All results lie between the generalizations for a vertical plate at laminar flow, proposed by Churchill and Chu [22], $Nu = 0.68 + 0.514Ra^{(1/4)}$, for air in a wide Ra range from 8×10^{-5} to $Ra_{cr} = 4 \times 10^8$ and that presented by Avduevsky and others [23], $0.80Ra^{(1/4)}$ for $Ra < 10^9$. A deviation from the power law (1/4) has been observed in favor of a law of (2/13).

Contrary to the horizontal position, at vertical position no significant distinction between cases A and B was detected.

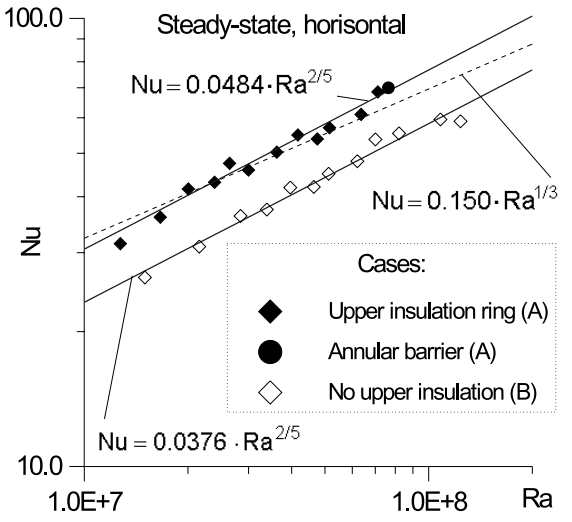

Fig. 5. Generalization of steady-state experimental data for horizontal position.

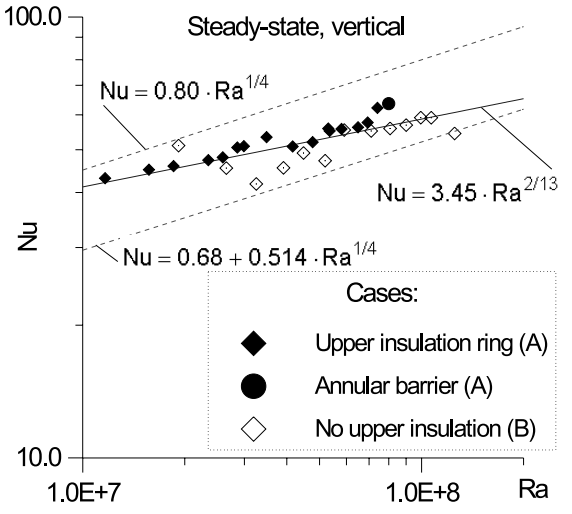

Fig. 6. Generalization of steady-state experiment data for vertical position.

The best expression obtained for vertical position in the range 1×10^7 to 2×10^8 is

$$Nu_D = 3.45 Ra_D^{(2/13)}. \quad (21)$$

A comparison of the results for these two positions displays the following. For small Ra from 1×10^7 to 3×10^7, heat transfer from vertical surface is higher than for horizontal. For Ra from 3×10^7 to 1×10^8 the Nu values are close to each other. For higher Ra the tendency looks like compliance to [24], where it was stated that heat transfer from horizontal surfaces is higher.

Experiments with a lateral annular barrier demonstrate no significant influence of such barrier on the heat transfer coefficient for both positions.

7. Experimental results of transient tests

Physically, the establishment of natural convection begins with the phase of pure heat conduction, when – transient phase, where the influence of edges and configuration peculiarities is significant and finally, steady-state convective cells are developed. The duration of each phase can be estimated by using the Zhukovsky criterion [1], $Zh = tv/L^2$.

In [27] transient effects were estimated. Experimental data were obtained for free convection of air under heating and cooling of a flat surface. The influence of unsteadiness is determined by the following dimensionless criterion

$$K_{T1} = \frac{\partial(T_w - T_\infty)}{\partial t} \sqrt{\frac{LT_m}{g}} (T_w - T_\infty)^{-3/2}. \quad (22)$$

The application of this criterion to the conditions of present experiment at $L \equiv D$ shows that the maximum value of this criterion about $K_{T1} \approx 0.1$ is reached at initiation of heating when the developed temperature difference is about 0.5°C. Throughout the entire cooling phase this criterion is small, $K_{T1} < -0.001$. According to [27,28] and by means of this criterion, the influence of unsteady does not exceed 1% and can be neglected at $\Delta T > 0.5$°C during heating phase and throughout whole cooling phase.

The purpose of the transient stage of this study is to refine the limits where the quasi-steady-state values of heat transfer coefficient can be used for the present conditions.

Each transient test consists of two phases: plate heating with the heaters switched on and cooling by natural convection with heaters switched off. Typical measured temperature profiles are shown in Fig. 7. As shown in the methodical section, each experimental curve is smoothed by a polynomial approximation. The power of approximation n is selected for each curve under the criterion when the average square residual is

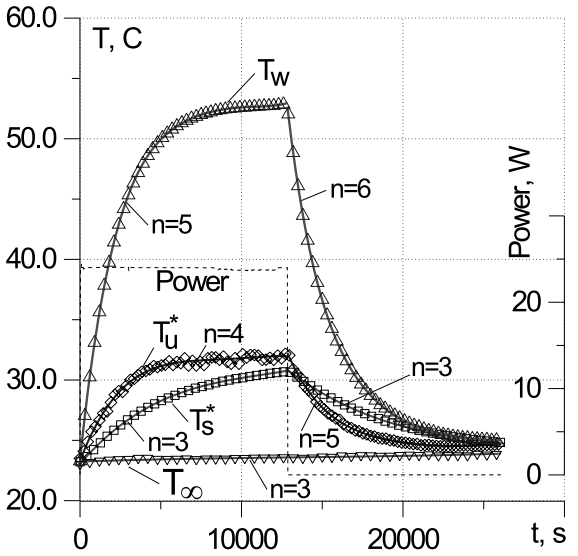

Fig. 7. Test profile. Case A (upper insulation ring), horizontal position, 24 W.

less than 0.0053(°C^2) for the plate and bottom insulation temperatures and less than 0.056 – for upper insulation.

Fig. 8 displays the generalization of the results obtained for the horizontal position of the base plate for the case B (without upper insulation ring). Curves were cut at low Ra numbers to fit an uncertainty ±15%, as defined in previous section. Results show that at the beginning of heating the value of transient $\alpha(t)$ lies below the quasi-steady-state values. It is in compliance with the general conception that heat transfer begins with conductive and subsequent transition phase. It is

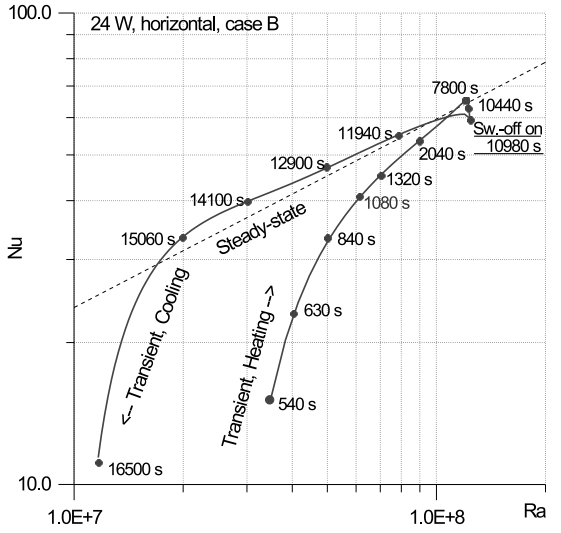

Fig. 8. Results of test at horizontal position, case B, 24 W.

also in qualitative compliance with the criterion K_{T1} but with the difference that the influence of the initial transient is still significant up to higher values of the developed temperature difference that is about 12–14°C. In the cooling phase, the deviation from the quasi-steady-state conception occurs at the end of the process, at a temperature difference close to 2–3°C. The maximal observed hysteresis related to the values of transient *Nu* for heating and cooling in the range of reliable data is 63%. The maximum temperature difference ΔT between the base plate and ambient is 22°C.

The influence of a lateral non-heated annular barrier of 150 mm of height was studied for horizontal position with an upper insulation ring. Obtained data presented in Fig. 9 demonstrate no practical influence of such barrier – the difference in *Nu* numbers does not exceed 6% that is similar to the steady-state case. It can be explained that permanent vertical oriented convective cells are formed above the plate and no lateral air supply is needed for the natural convection. This result is similar to that obtained for smooth rectangular surfaces, presented in [11,12].

For the case A (upper insulation ring) the hysteresis between magnitudes of $Nu(t)$ in heating and cooling phases is presented too, such as for the case B, but the value appears to be smaller. The maximum observed hysteresis is 41%, but the range of reliable data for the case A is narrower than for case B, as it is stated in previous section.

Fig. 10 shows the generalization of the transient test at vertical position for the case A at different heat dissipation. The values of hysteresis are varied in the range from 59% to 73%, the higher the lower the heat dissipation.

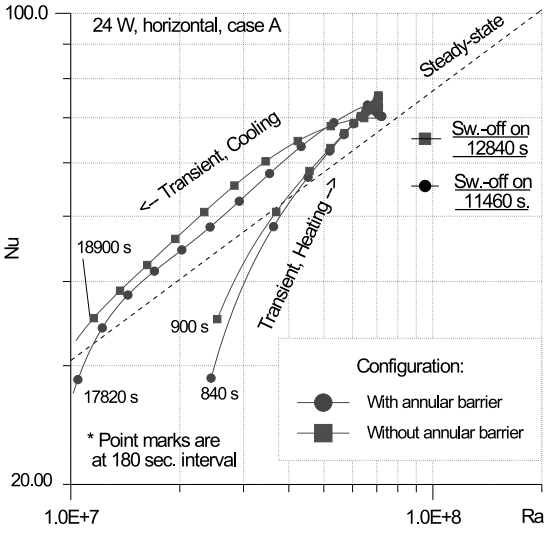

Fig. 9. Test data for different configurations.

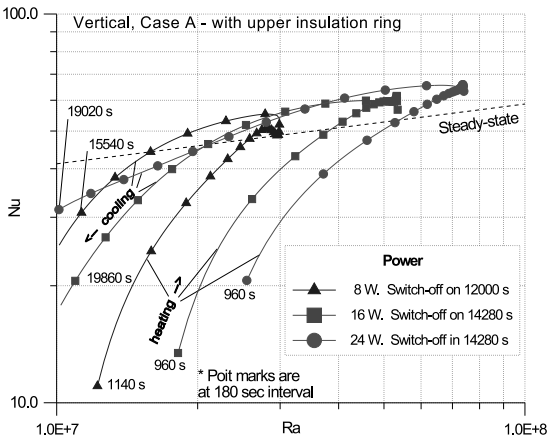

Fig. 10. Results of test in vertical position at different heat dissipations, case A.

Tests with a lateral non-heated annular barrier at vertical position show that such barrier does not affect the heat transfer, similar to the case of horizontal position. It can be explained that this barrier has a larger diameter (504 mm) than the base plate surface (384 or 293 mm). This distance seems sufficient to smooth perturbations of overall laminar flow in upward direction.

8. Conclusion

The investigations conducted for the plate of complex configuration showed that the intensity of natural convective heat transfer and radiation at steady state can be evaluated by the relations obtained for classic smooth surfaces of simple configuration (round or quadrate) within the range of 26%. For more precise estimation the following peculiarities should be taken into account. Some obstacles like insulation inserts in the central region of a round plate in horizontal plate position can interfere development of vertical vortices and provoke a slight modification in the power law for turbulent flow from (1/3) to (2/5).

An upper insulation ring in the perimeter region of the round plate eliminates some adverse edge effects and simultaneously acts as a turbulizer intensifying convective heat transfer. Observed difference between the cases of with and without upper insulation is of 22% for horizontal position.

At vertical position, an upper insulation ring does not yield such influence like for horizontal case due to different mechanism of convective heat transfer. The insulation inserts in the central region of the plate in vertical position modify the power law for laminar flow from (1/4) to (2/13).

Comparison of convective heat transfer coefficients for two horizontal and vertical positions demonstrates that for the condition of the present experiment its ratio depends on the *Ra* number. For small *Ra* (1×10^7 to 3×10^7), heat transfer is more intensive for vertical position of the plate; for *Ra* (3×10^7 to 1×10^8) the *Nu* values are close to each other and for higher *Ra* the tendency looks like this coefficient is higher for the horizontal position.

An annular barrier that bounded the base plate around perimeter with some distance has no influence on heat transfer at any position of the plate for steady-state tests as well as for transient.

Through transient tests a distinguished reduction in heat transfer compared to quasi-steady-state values was observed at the beginning of heating phase and at the end of cooling phase. At the beginning of heating phase, when the developed temperature difference ΔT between the base plate and ambient is of 27–36% of maximal steady state difference for certain level of power dissipated, the reduction in convective heat transfer is of 31–75%. When the temperature difference becomes about 65% of maximal, the quasi-steady-state conception appears to be valid.

Cooling phase appears to be more compliant with quasi-steady-state conception for most tests. The deviation from steady-state values occurs at the end of the cooling phase when the developed temperature difference between the base plate and ambient is of 14–36% of maximal steady state difference, depending on maximal power dissipated.

A clear hysteresis between heating and cooling phases was detected for most transient tests. The hysteresis ratio between values of the *Nu* number for the heating and cooling phases at the same values of the *Ra* number were varied in the range from 59% to 73%, the higher the lower the heat dissipation. High ratio of the hysteresis was observed for the case B in horizontal position, lower ratio for the case A in both horizontal and vertical positions and the hysteresis almost disappeared for the case B at vertical position.

Acknowledgements

The authors are very grateful to the Conselho Nacional de Desenvolvimento Cientifico e Tecnologico – CNPq, of Brazilian Government for the financial support received through the grant number 300327/90-4(NV).

References

[1] O.G. Martynenko, Y.A. Sokovishin, Natural Convection Heat Transfer, Handbook, Nauka i tekhnika, Minsk, 1982.

[2] B. Gebhart, Y. Jaluria, R.L. Mahejan, R. Sammakia, Buoyancy-induced Flows and Transport, Hemisphere, London, 1988.

[3] J.A. Schetz, R. Eichorn, Natural convection with discontinuous wall-temperature variations, J. Fluid Mech. 18 (2) (1964) 167–176.

[4] A.A. Hayday, D.R. Bowlus, R.A. McGrow, Natural convection on a vertical flat surface with stepped temperature profile, Trans. ASME, J. Heat Transfer 89 (1967) 244.

[5] M.D. Kellehar, Natural convection from vertical surface at explosive character of wall temperature, Trans. ASME, J. Heat Transfer 93 (1971) 349.

[6] K. Kishinami, N. Seki, Natural convection heat transfer near vertical adiabatic surface located above isothermal surface, Trans. ASME, J. Heat Transfer 105 (1983) 759.

[7] B.H. Kang, Y. Jaluria, Natural convection heat transfer characteristics of a protruding thermal source located on horizontal and vertical surfaces, Int. J. Heat Mass Transfer 33 (1990) 1347–1357.

[8] R.F. Boehm, D. Kamayab, Established stripwise laminar natural convection on a horizontal surface, Trans. ASME 99 (C2) (1977) 293–298.

[9] W. Jasinski, Eksperimentalne badanie ciepla na poziomych plitach nieizotermicznych w warunkach konwekcji swobodnej, W.: Ref. Sympoz. wymiany ciepla i masy, Warszawa-Jablonma, 1976, pp. 145–151.

[10] I.A. Clarc, Cryogenic heat transfer, in: Advances in Heat Transfer, vol. 5, Academic Press, New York, 1968, pp. 325–517.

[11] H.R. Jacobs, W.E. Mason Jr., Natural convection in open rectangular cavities with adiabatic sidewalls, in: Proceedings of the 1976 Heat Transfer and Fluid Mechanics, Inst. Stanford, 1976, pp. 33–46.

[12] H.R. Jacobs, W.E. Mason Jr., E.T. Hikida, Natural convection in open rectangular cavities, in: Proceedings of the 5th International Heat Transfer Conference, vol. 3, Tokyo, 1974, pp. 89–93.

[13] R. Piva, P. Orlandi, Numerical solution for flow in atmospheric boundary layer in canyon, in: Numerical Solution of Hydrodynamic Problems. Moscow, 1977, pp. 127–134.

[14] I. Sezai, A.A. Mohamad, Suppressing free convection from a flat plate with poor conductor ribs, Int. J. Heat Mass Transfer 42 (1999) 2041–2051.

[15] C.K. Hsieh, R.W. Coldewey, The natural convection of air over a heated plate with forward-facing step, Trans. ASME, J. Heat Transfer 99 (C3) (1977) 439–445.

[16] V.P. Ivakin, A.N. Kekalov, Influence of steps on natural convection heat transfer in vertical boundary layer, in: Some Problems of Hydrodynamics and Heat Transfer, Novosibirsk, 1976, pp. 23–28.

[17] M. Al-Arabi, M.K. El-Riedy, Natural convection heat transfer from isothermal horizontal plates of different shapes, Int. J. Heat Mass Transfer 19 (12) (1976) 1399–1404.

[18] R.V. Rammohan, C. Balaji, S.P. Venkateshan, Interferometric study of interaction of free convection with surface radiation in an L corner, Int. J. Heat Mass Transfer 40 (1997) 2941–2947.

[19] N. Ramesh, S.P. Venkateshan, Effect of surface radiation and partition resistance on natural convection heat transfer

in a partitioned enclosure: An experimental study, J. Heat Transfer 21 (1999) 616–622.
[20] B. Gebhart, Surface temperature calculations in radiant surroundings of arbitrary complexity – for gray, diffuse radiation, Int. J. Heat Mass Transfer 3 (4) (1961) 341–346.
[21] M. Fishenden, O.A. Saunders, An Introduction to Heat Transfer, Oxford University Press, London, 1950.
[22] S.W. Churchill, H.H.S. Chu, Correlation equations for laminar and turbulent free convection from a vertical plate, Int. J. Heat Mass Transfer 18 (11) (1975) 1323–1329.
[23] V.S. Avduevsky, B.M. Galitsevski, G.A. Glebov, G.A. Dreitser, Fundamentals of Heat Transfer in Aviation and Rocket – Space Technics, Textbook, second ed., Mashinostroenie, Moscow, 1992.
[24] M. Mikheev, Fundamentals of Heat Transfer, Mir, Moscow, 1968.
[25] M. Özişik, Heat Conduction, Wiley, New York, 1980.
[26] J.V. Beck, K.D. Cole, A. Haji-Sheikh, B. Litkouhi, Heat Conduction Using Green's Functions, Hemisphere, London, 1992.
[27] E.K. Kalinin, G.A. Dreitser, A.S. Neverov, Experimental study of unsteady heat transfer of natural gas convection near vertical tube, in: Anthology: Hidravlika, Trudy VZMI, Works of All-Union Correspondence Mashine-Building Institute, Moscow, 1976.
[28] E.K. Kalinin, G.A. Dreitser, Unsteady convective heat transfer in channels, in: Advances in Heat Transfer, vol. 25. Academic Press, New York, 1994, pp. 1–150.
[29] G.A. Dreitser, Fundamentals of Convective Heat Transfer in Channels Textbook, Moscow Aviation Institute, Moscow, 1989.